Transactions on Biomedicine and Health vol 2, © 1995 WIT Press, www.witpress.com, ISSN 1743-3525

Solving the inverse problem of electrocardiology using body surface Laplacian mapping

P.R. Johnston
Department of Medicine, University of Tasmania,
43 Collins Street, Hobart, Tasmania 7000, Australia

Abstract

The determination of epicardial potentials is very important in the diagnosis of various cardiac disorders. It has been common practice to calculate these potentials from potentials measured on the body surface and then use a regularisation technique, such as that due to Tikhonov. Here it will be demonstrated that these same potentials can be determined using the recently described body surface Laplacian maps.

Using a concentric spheres model, for which the surface Laplacian can be calculated analytically, a transfer matrix is calculated relating epicardial potentials to the Laplacian of the body surface potentials. The epicardial potentials are recovered by inverting this transfer matrix with the usual Tikhonov regularisation technique.

From our initial work in this area, the determination of epicardial potentials from body surface Laplacian maps is markedly superior to those from potential measurements.

1 Introduction

The cardiac electric field can be noninvasively studied by mapping the cardiac electrical activity on the surface of the body. These body surface potential maps have been studied extensively over the past thirty or more years in an attempt to obtain spatial information on cardiac electric sources. Almost hand in hand with these studies, attempts have been made to directly visualise the epicardial potential distribution using inversion techniques (Gulrajani et al., [1]). Unfortunately, this type of inversion is ill–posed and

susceptible to errors in both the numerical solution of the forward problem and measurement of the potential. The usual method to minimise these errors is to use a form of Tikhonov regularisation (Tikhonov and Arsenin, [2]).

Recently, a technique has been proposed which is able to measure the Laplacian of the surface potentials by means of a concentric bipolar electrode (He and Cohen, [3]). That is, the Laplacian is estimated as the potential difference between a central electrode and an annular ring encompassing this circular electrode. It is demonstrated (He and Cohen, [3]) that the Laplacian map can better image spatially distributed dipole sources, in a half conductor, than the potential map. These maps have also been used to resolve polarisation and depolarisation of different regions of the heart in a normal human (He and Cohen, [3]), as well as identifying the pacemaker focus and activation sequence from exogenous ventricular pacing in pigs (He et al., [4]).

2 Concentric Spheres Model

A simple but realistic approach to demonstrate the inversion procedure is to consider two concentric spheres. Here, Laplace's equation of the three dimensional case in spherical coordinates is

$$\frac{1}{r^2}\frac{\partial}{\partial r}\left(r^2\frac{\partial u}{\partial r}\right)+\frac{1}{r^2\sin(\theta)}\frac{\partial}{\partial\theta}\left(\sin(\theta)\frac{\partial u}{\partial\theta}\right)+\frac{1}{r^2\sin^2(\theta)}\frac{\partial^2 u}{\partial\phi^2}=0 \qquad (1)$$

where (r,θ,ϕ) are the usual spherical coordinates. The boundary condition on the outer sphere is that there is no current flow to the outside

$$\frac{\partial u}{\partial r}=0 \quad \text{at} \quad r=1 \qquad (2)$$

Also required is a specified potential distribution on the inner surface

$$u=h(\theta,\phi) \quad \text{at} \quad r=R \qquad (3)$$

for some $0<R<1$.

Solving the above equation, subject to the boundary conditions, via separation of variables gives the following solution for the potential on the outer surface

$$\begin{aligned} u(1,\theta,\phi) &= \frac{A_{00}}{4\pi}+\frac{1}{4\pi}\sum_{m=1}^{\infty}\frac{(2m+1)^2A_{0m}}{(m+1)R^m+mR^{-(m+1)}}P_m^0(\cos(\theta)) \\ &+ \frac{1}{2\pi}\sum_{m=1}^{\infty}\frac{(2m+1)^2}{(m+1)R^m+mR^{-(m+1)}} \\ &\times \sum_{n=1}^{m}\frac{(m-n)!}{(m+n)!}\left(A_{nm}\cos(n\phi)+B_{nm}\sin(n\phi)\right)P_m^n(\cos(\theta)) \end{aligned} \qquad (4)$$

where

$$\begin{aligned} A_{00} &= \int_0^{\pi}\int_0^{2\pi} h(\theta,\phi)d\phi d\theta \\ A_{0m} &= \int_0^{\pi}\int_0^{2\pi} h(\theta,\phi)P_m^0(\cos(\theta))\sin(\theta)d\phi d\theta \\ A_{nm} &= \int_0^{\pi}\int_0^{2\pi} h(\theta,\phi)\cos(n\phi)P_m^n(\cos(\theta))\sin(\theta)d\phi d\theta \\ B_{nm} &= \int_0^{\pi}\int_0^{2\pi} h(\theta,\phi)\sin(n\phi)P_m^n(\cos(\theta))\sin(\theta)d\phi d\theta \end{aligned}$$

The Laplacian of the outer surface potentials is obtained by evaluating the Laplacian operator from Equation (1) ar $r = 1$ and is given by

$$\nabla_s^2 u(1,\theta,\phi) = \frac{1}{\sin(\theta)}\frac{\partial}{\partial\theta}\left(\sin(\theta)\frac{\partial u}{\partial\theta}\right) + \frac{1}{\sin^2(\theta)}\frac{\partial^2 u}{\partial\phi^2} \tag{5}$$

as there is no radial variation in surface potential. Applying this operator to the outer surface potential distribution, Equation (5), gives

$$\begin{aligned} \nabla_s^2 u(1,\theta,\phi) &= -\frac{1}{4\pi}\sum_{m=1}^{\infty}\frac{m(m+1)(2m+1)^2 A_{0m}}{(m+1)R^m + mR^{-(m+1)}}P_m^0(\cos(\theta)) \\ &+ \frac{1}{2\pi}\sum_{m=1}^{\infty}\frac{m(m+1)(2m+1)^2}{(m+1)R^m + mR^{-(m+1)}} \\ &\times \sum_{n=1}^{m}\frac{(m-n)!}{(m+n)!}\left(A_{nm}\cos(n\phi) + B_{nm}\sin(n\phi)\right)P_m^n(\cos(\theta)) \end{aligned} \tag{6}$$

To determine a forward transfer matrix for both the potential and the Laplacian, the outer surface is assumed to be approximated by p nodes and the inner surface by q nodes, where $q < p$. Each row of the transfer matrix is calculated by evaluating the coefficients assuming that $h(\theta,\phi)$ is a two dimensional Dirac delta function at a given node on the inner surface, and obtaining the resulting potential or Laplacian at each node on the outer surface.

3 The Inversion Process

At this stage, forward transfer matrices have been obtained which relate the inner surface potential to both the outer surface potential and its Laplacian. Mathematically, the first relationship can be represented by

$$\mathbf{A}h = b \tag{7}$$

where h is the vector of inner surface potentials, b the vector of outer surface potentials and $\mathbf{A}$ the forward transfer matrix for the potentials. The second relationship can be expressed as

$$\mathbf{B}h = l \tag{8}$$

where l is the vector of outer surface Laplacians and $\mathbf{B}$ is the forward transfer matrix for the Laplacians. The common factor between these two equations is the vector of inner surface potentials, h, which, in principle, can be determined by a knowledge of either the body surface potentials or its Laplacian.

The usual method of recovering the vector h, given the potential vector b, is to use a form of Tikhonov regularisation. Here zero–order Tikhonov regularisation is used where the functional

$$M_t(h) = \|\mathbf{A}h - b\|^2 + t\|h\|^2 \tag{9}$$

is minimised, giving the solution

$$h_t = (\mathbf{A}^t\mathbf{A} + t\mathbf{I})^{-1}\mathbf{A}^t b \tag{10}$$

where $\mathbf{I}$ is an appropriately sized identity matrix. The parameter $t(> 0)$, known as the regularisation parameter, weights the norm of the residual against the norm of the solution itself. Since Equation (8) is of the same form as Equation (7), it seems reasonable to solve this equation also using zero–order Tikhonov regularisation. Therefore, the functional

$$N_s(h) = \|\mathbf{B}h - l\|^2 + s\|h\|^2 \tag{11}$$

is to be minimised, giving the solution

$$h_s = (\mathbf{B}^t\mathbf{B} + s\mathbf{I})^{-1}\mathbf{B}^t l \tag{12}$$

where $s(> 0)$ is another regularisation parameter which weights the norm of the inner surface potentials against the norm of the difference between predicted and observed outer surface Laplacians.

4 Methods of Comparison

One method to compare the effectiveness of these two inversion methods is to use the concept of the trade–off curve (Johnston et al., [5]). A trade–off curve consists of a plot of spread versus average noise amplification factor, n_a, where each point on the curve is determined by calculating the spread and n_a for a given regularisation parameter. Both the spread and n_a are

calculated from a $p \times q$ forward transfer matrix, $\mathbf{T}$, and are defined as follows:

$$spread(\mathbf{T}) = \|\mathbf{T}^{-g}\mathbf{T} - \mathbf{I}\|_F^2 \tag{13}$$

and

$$n_a = \frac{1}{q}\sum_{i=1}^{q}\sqrt{\sum_{j=1}^{p}(\mathbf{T}^{-g})_{ij}^2} \tag{14}$$

respectively, where $\|\cdot\|_F$ is the Frobenius norm.

In these formulae, the quantity $\mathbf{T}^{-g}$ is the generalised inverse of the matrix $\mathbf{T}$ and for the two cases considered in the previous section

$$\mathbf{A}^{-g} = (\mathbf{A}^t\mathbf{A} + t\mathbf{I})^{-1}\mathbf{A}^t \tag{15}$$

and

$$\mathbf{B}^{-g} = (\mathbf{B}^t\mathbf{B} + s\mathbf{I})^{-1}\mathbf{B}^t \tag{16}$$

The spread measures the amount of information contained in the neighbours of a given node on the inner surface. The smaller the spread (obtained for small values of the regularisation parameter), the greater the reliability placed on the results. On the other hand, larger values of the spread indicate that the inversion process has smeared the potential over the inner surface. The noise amplification gives a measure of how the inversion process magnifies the errors in the data collection process. Small values of n_a mean that errors in data collection are less likely to affect the overall solution, but this is usually achieved at the expense of great smearing of the inner potential. The inversion process represents a trade-off between these two quantities.

The other use for these curves is to compare two different transfer matrices. For each matrix a trade-off curve can be plotted and the curve which lies closest to the axes indicates that its associated inverse transfer matrix is the more stable and reliable in the inversion process.

The correctness of an inversely calculated inner surface potential distribution compared to its original distribution can be measured by either the relative error, RE, namely,

$$RE = \frac{\|h - h_I\|}{\|h_I\|} \tag{17}$$

or the correlation coefficient, CC, given by

$$CC = \frac{\sum_{j=1}^{q}[h_j - \overline{h}][(h_I)_j - \overline{h_I}]}{\|h - \overline{h}\|\|h_I - \overline{h_I}\|} \tag{18}$$

In these definitions, h_I represents the initial, known inner surface distribution and h represents the computed one. The quantities $\overline{h_I}$ and $\overline{h}$ are, respectively, the mean values of h_I and h, over the q inner surface nodes.

5 Simulations

Simulations of two different types were performed. Firstly, trade–off curves were plotted for the potential and Laplacian forward transfer matrices. Secondly, the full inversion procedure was tested using analytically determined inner surface potentials and outer surface potentials and Laplacians resulting from a finite number of radial dipoles within the inner sphere. In all simulations, and to be somewhat representative of the human torso, the radius of the outer surface was given the value of unity and the radius of the inner surface was set to 0.4.

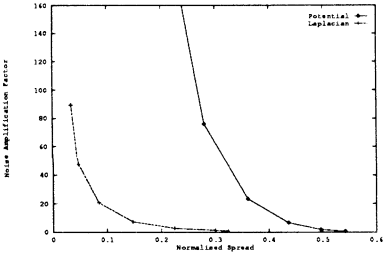
In the concentric spheres model, the inner surface was approximated by 218 nodes and the outer surface by 866 nodes, resulting in transfer matrices of size 866×218 for both the potential and Laplacian. The ratio of approximately 4:1, for the number of outer nodes to inner nodes, was chosen to comply with that previously suggested (Johnston et al., [5]).

6 Results and Discussion

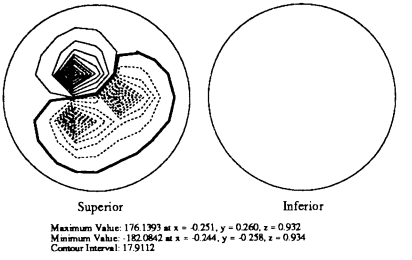
Two forward transfer matrices corresponding to the potential and Laplacian forward problems were created as discussed in the previous section. For each of these matrices a trade–off curve was produced and these are plotted in Figure 1(a). The value of the spread has been divided by the number of nodes on the inner surface (218) to normalise it between 0 and 1. A spread of 0 would indicate that the inner surface potentials had been uniquely determined while, on the other hand, a spread of 1 means that the potential at each node would contain some information from every other node on the surface.

From Figure 1(a), it can be seen that the trade–off curve for the Laplacian forward transfer matrix is much closer to the axes than that of the potential forward transfer matrix. This means that given the same noise level for both the potential and Laplacian measurements, the calculated inner surface potentials are less likely to be smeared across the inner surface. Even if there is slightly greater noise on the Laplacian measurements over the potential measurements, a smaller spread will still result for the inverse solution obtained from the Laplacian than that obtained from the potential measurements.

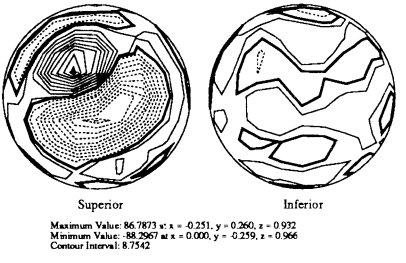
The remaining three panels in Figure 1 show inner surface potential distributions. Panel (b) is the initial distribution arising from three radial dipoles within the inner sphere. Note the three extrema and the high potential gradients. Panel (c) is the distribution calculated from outer surface potential measurements with 2% added noise and panel (d) is the distribution calculated from outer surface Laplacian measurements with 5% added



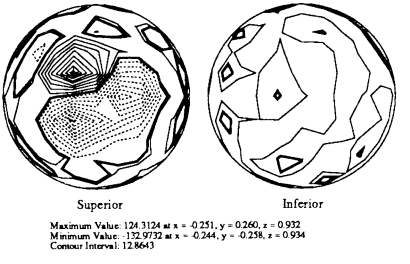
(a) Trade–off Curves



(b) Input Heart Surface Distribution



(c) Heart Surface Distribution Calculated from Potentials with 2% Noise



(d) Heart Surface Distribution Calculated from Laplacians with 5% Noise

Figure 1: Results from Concentric Spheres Simulation

noise. Observe that the Laplacian measurements are able to extract the three extrema and recover the high potential gradients (even in the presence of higher added noise), whereas the potential measurements cannot. Also, the values of the inner surface potential calculated from the Laplacian measurements are much closer to the original values than those calculated from the potential measurements.

These simulations show that it is possible to solve the inverse problem of electrocardiology (albeit in a simple approximation) from a knowledge of the Laplacian of the outer surface potential distribution. Inner surface potentials obtained, using zero order Tikhonov regularisation, from measurements of the Laplacian are superior to those obtained, also with zero order Tikhonov regularisation, from measurements of the potential, even in the presence of measurement noise.

The trade–off curves (Figure 1(a)) suggest that there can be greater noise in the Laplacian measurements than in the potential measurements and still obtain superior inverse solutions. This fact is also borne out by considering the condition numbers for the forward transfer matrices. The condition

number for the potential forward transfer matrix was 2.83×10^7 and for the Laplacian forward transfer matrix it was 1.34×10^5. Hence, it can be seen that the Laplacian forward transfer matrix is less ill-conditioned than the potential forward transfer matrix. In turn, this means that the Laplacian inverse problem is less sensitive to errors in measurement than the potential inverse problem and so greater errors are allowed in measuring the surface Laplacians to achieve similar results from potential measurements. For example, if there is an order of magnitude greater noise level on the Laplacian measurements over the potential measurements (say 20% compared to 2%), then to achieve the same error level on the inner surface a noise amplification factor one order of magnitude smaller would be required for the Laplacian inverse. It can be seen from Figure 1(a) that this smaller n_a results in a smaller spread for the inverse solution obtained from the Laplacian than that obtained from the potential measurements. Therefore, the inner surface potential obtained from measurements of the Laplacian would be more accurate than those obtained from measuring the surface potential, even with significantly greater noise in the original measurements. When 20% noise was added to the Laplacian measurements in the second simulation, the optimal parameters where $RE = 0.492$ and $CC = 0.871$ at $s = 10^{-2}$, which are superior to those obtained from the potential measurements with only 2% noise ($RE = 0.526$ and $CC = 0.851$ at $t = 10^{-5}$).

Acknowledgement:- This work was funded by the Australian Research Council.

References

[1] Gulrajani, R. M., Roberge, F. A., and Savard, P. *The inverse problem of electrocardiology*, volume 1 of *Comprehensive Electrocardiology*, chapter 9, pages 237–288. Pergamon Press, first edition, 1989.

[2] Tikhonov, A. N. and Arsenin, V. Y. *Solutions of Ill-Posed Problems*. V. H. Winston and Sons, Washington, 1977.

[3] He, B. and Cohen, R. J. Body surface Laplacian ECG mapping. *IEEE Trans. Biomed. Engng.*, Vol. 39(11), pp. 1179–1191, November 1992.

[4] He, B., Kirby, D. A., Mullen, T., and Cohen, R. J. Body surface Laplacian ECG mapping of cardiac excitation in intact pigs. *PACE*, Vol. 16, pp. 1017–1026, 1993.

[5] Johnston, P. R., Walker, S. J., Hyttinen, J. A. K., and Kilpatrick, D. Inverse electrocardiographic transformations: Dependence on the number of epicardial regions and body surface data points. *Math. Biosci.*, Vol. 120(2), pp. 165–187, April 1994.